

Chapter 1

Position of the Reverberation Chambers in Common Electromagnetic Tests

1.1. Introduction

In addition to the conduction tests, the common immunity or emission tests required in electromagnetic compatibility involve the production of electric fields of an amplitude higher than 1 V/m, or on the contrary the measurement of low fields, whose amplitude can be close to 100 $\mu\text{V/m}$.

The use of the electromagnetic plane wave concept offers experimenters the means to qualify most of the devices as tests recommended by international standards or conceived for specific applications. The plane wave is based on a theoretical ideal stating that no experiment can rigorously reproduce. Paradoxically, we will see in this first chapter and the subsequent stages of the book, that it is the confrontation of the plane wave concept that allows us quite frequently to appreciate the reproducibility criteria of a test.

The estimate of the error margins is thus the major concern during the design of new test methods or during the improvement of the existing test methods.

These reasons have thus encouraged us to write the first section of this chapter about the theoretical concepts of plane waves. Although generally confused with the ray propagation adopted in geometrical optics methods, the plane wave has significantly different physical properties. The particularity of the plane wave is above all due to the polarization plane perpendicular to the propagation direction of

2 Electromagnetic Reverberation Chambers

the wave. Another property is added to this first property, stipulating that the orthogonal electric field \vec{E} and magnetic field \vec{H} vectors carried by the wave, remain invariant for an observer moving in the polarization plane. Moreover, thanks to the resolution of Maxwell's equations in a vacuum, one shows that the ratio of the amplitudes of \vec{E} and \vec{H} corresponds to the square root of the ratio of the absolute magnetic permeability μ_0 and the absolute electric permittivity ϵ_0 . This is the impedance of the plane wave, approximately taking the real value of 377Ω .

The following section will be concerned with the examination of the physical behavior of objects submitted to tests done in a TEM cell and in an anechoic shielded chamber. With the help of an object reduced to a small magnetic loop, several sources of uncertainties will be identified. They result from the imperfections of the instruments and from the environment of the object under test. The open discussion on the contribution of these uncertainties will lead to the physical principle of mode-stirred reverberation chambers. Contrary to the methods previously described, reverberation chambers directly introduce, from their functioning principle, uncertainties which may be characterized by statistical analysis. These properties will be implemented in the calibration protocols, which will guarantee the reproducibility of the tests carried out in chambers of various volumes and constitution.

1.2. Electromagnetic fields and plane waves

In accordance with the predictions of the J.C. Maxwell equations, established at the end of the 19th Century, the electromagnetic waves are recounted by a propagation phenomenon in the space linking an electric field vector \vec{E} and a magnetic field vector \vec{H} . In the current system of standardized units, electric and magnetic field are respectively expressed in V/m and A/m . The most known effects generated by the fields are expressed in terms of currents or voltages induction, appearing in the electric circuits exposed to the waves and that we generally call electromagnetic interferences. Implementing an electromagnetic test will thus consist of the measurement of the field amplitude and of the effects consecutive to the induction phenomena that they produce.

The most elementary representation of an electromagnetic wave is made up of the *plane wave*, whose properties are close to the ray propagation in optics. Most of the tests designed to evaluate the behavior of electronic equipment exposed to fields animated by sinusoidal amplitude variations are also based on the notion of plane waves. The formalism of plane waves also concerns the undesirable electromagnetic fields emitted by this equipment, while these are operated in usual conditions.

In the context of electromagnetic compatibility, the analysis of the behavior of electronic equipment subjected to an electromagnetic field will concern *immunity* or *susceptibility* tests.

The immunity is the aptitude of a device to operate without fault, when it is exposed to electromagnetic interference, whose physical characteristics have been specified beforehand by a measurement protocol. Susceptibility tests are designed to determine the parameters of the interference causing faulty functioning of this same device.

The emission measurement relates to the evaluation of the electromagnetic fields or to the interference level that electronic equipment can produce in its close environment during use. To carry out an emission measurement thus consists of determining the fields' amplitude observed on the electromagnetic spectrum, generated by this equipment and at a distance specified by an appropriate protocol [HAR 61].

1.2.1. Definition and properties of plane waves

Let us consider the geometrical Cartesian graph xyz shown in Figure 1.1.

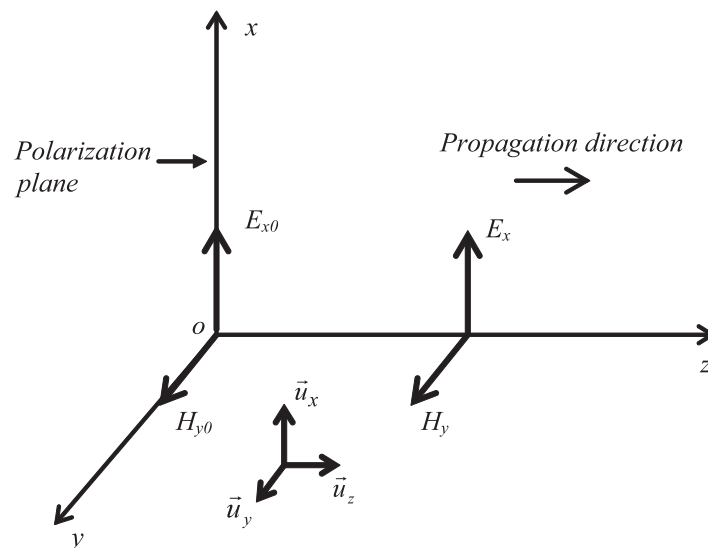


Figure 1.1. Cartesian geometrical references of a plane wave

4 Electromagnetic Reverberation Chambers

The plane wave is made up of vector functions $\vec{e}(z,t)$ and $\vec{h}(z,t)$ dependent on the space variable z and on the time variable t . Knowing that this wave will then be animated by sinusoidal amplitude variations with the time variable, their representation in the diagram of Figure 1.1 can be reduced to the maximal, root mean square (rms) or complex amplitudes alone, designated by an upper-case syntax.

With the previous assumptions, we associate with the plane wave two amplitude vectors of electric \vec{E} and magnetic \vec{H} orthogonal fields. The plane containing the vectors \vec{E} and \vec{H} is called the *polarization plane*. The plane wave is such that the amplitude and direction of the vectors \vec{E} and \vec{H} remain invariant in the polarization plane; *the propagation direction* of the wave is perpendicular to the polarization plane.

For the example illustrated in Figure 1.1, the polarization plane is merged with the oxy graph, and the propagation direction is contained on the oz axis perpendicular to the previous graph. When the propagation has the same direction as the oz axis, it is a forward wave and when the propagation is in the opposite direction, it is a backward wave. The use of unit vectors (at the bottom of Figure 1.1) leads to \vec{E} and \vec{H} , expressed under the forms:

$$\vec{E} = E_x \vec{u}_x \quad \vec{H} = H_y \vec{u}_y \quad [1.1]$$

1.2.1.1. Waves equations

From the development of Maxwell equations, we manage to link \vec{e} and \vec{h} to the variables z and t by the following waves equations:

$$\frac{\partial^2 \vec{e}}{\partial z^2} - \frac{1}{v_0^2} \frac{\partial^2 \vec{e}}{\partial t^2} = 0 \quad \frac{\partial^2 \vec{h}}{\partial z^2} - \frac{1}{v_0^2} \frac{\partial^2 \vec{h}}{\partial t^2} = 0 \quad [1.2]$$

The v_0 parameter represents the propagation speed in the considered environment; if the wave propagates in a vacuum, v_0 is the speed of light in vacuum so-called celerity c . An expression close to c can be established with the help of the absolute magnetic permeability of the vacuum μ_0 and of the electric permittivity ϵ_0 , i.e.:

$$v_0 = c = \frac{1}{\sqrt{\mu_0 \epsilon_0}} \quad [1.3]$$

We will recall the values of μ_0 and ε_0 , expressed in the standardized units system:

$$\mu_0 = 4\pi 10^{-7} \text{ H / m} \quad \varepsilon_0 = \frac{1}{36\pi} 10^{-9} \text{ F / m} = 8.841941 10^{-12} \text{ F / m} \quad [1.4]$$

Formulation of expressions [1.2] and [1.3] calls for two comments. Indeed, contrary to common usage, we have called [1.2] a waves equation, using the plural. We think it is preferable in the context of the subject discussed in this book. As we will see later on, equation [1.2] will generate eigenvalues expressing an infinite spectrum of standing waves. Moreover, the celerity calculated by expression [1.3] from the absolute electric permittivity, given by the usual formula [1.4], is significantly incorrect. Indeed, the value of the speed of light in a vacuum is set by decree since 1983 at 299,792,458 m/s. This legal provision is justified by the definition of the meter established on the basis of the time unit (the second), precisely set by atomic clocks. Consequently, to exactly know the celerity using equation [1.3], we need to enter for ε_0 the value: $8.854187 \cdot 10^{-12}$ F/m [ESU 05, UZA 05].

1.2.1.2. Relations linking the electric and magnetic fields

Maxwell's equations lead to mutual calculations of the electric and magnetic fields. For the wave presented in Figure 1.1, the relations take the forms:

$$-\frac{\partial e_x}{\partial z} = \mu_0 \frac{\partial h_y}{\partial t} \quad -\frac{\partial h_y}{\partial z} = \varepsilon_0 \frac{\partial e_x}{\partial t} \quad [1.5]$$

1.2.1.3. Plane waves animated by continuous harmonic variations

The sources generating electromagnetic fields, adopted in immunity or susceptibility tests, generally release sinusoidal signals of angular frequency ω . By admitting the linear functioning of the emitter, the amplitude fluctuations of the vectors \vec{e} and \vec{h} remain sinusoidal and incidentally out of phase compared to the generator signal.

Using complex notations highly simplifies the link between \vec{e} and \vec{E} , where the projections of the vector \vec{E} then include complex functions of the space variables x , y , and z :

$$\vec{e}(x, y, z, t) = \vec{E}(x, y, z) e^{j\omega t} \quad [1.6]$$

A similar convention is applied to the magnetic field vector.

1.2.1.4. *Resolution of the waves equation*

With the hypothesis of the representation in Figure 1.1 and of the harmonic variations formulated in [1.6], the waves equation will be expressed as [1.7] in which we introduce the k coefficient, called the wave number. The wave number represents the ratio between the angular frequency ω of the wave and its propagation speed v_0 :

$$\frac{d^2 \vec{E}}{dz^2} + k^2 \vec{E} = 0 \quad \text{where} \quad k = \frac{\omega}{v_0} \quad [1.7]$$

The resolution of this equation designed in free-space leads to solution [1.8], where the term E_{x0} corresponds to the complex amplitude of the wave, defined at the origin of the graph in Figure 1.1:

$$E_x = E_{x0} e^{-jkz} \quad \text{with} \quad \vec{E} = E_x \vec{u}_x \quad [1.8]$$

The obtained solution shows that the absolute amplitude of the field E_x remains invariant during the propagation, whereas the phase shows a delay proportional to the space variable z , i.e.:

$$|E_x| = E_{x0} \quad \text{and} \quad \phi[E_x] = kz \quad [1.9]$$

1.2.1.5. *Wavelength*

The phase term in equation [1.9] can be presented differently by making the product 2π with the ratio made up of the variable z and a quantity λ (the wavelength) appear. We thus easily link the wavelength to the parameters k , ω , and to the frequency f by the relation on the right in [1.10]:

$$\phi[E_x] = 2\pi \frac{z}{\lambda} \rightarrow k = \frac{2\pi}{\lambda} \rightarrow \lambda = \frac{v_0}{f} \quad \text{where} \quad \omega = 2\pi f \quad [1.10]$$

1.2.1.6. *Impedance of the plane wave*

With the use of equation [1.5], we deduce for the function $\vec{h}(z, t)$, a form strictly identical to the solution of the electric field. The ratio of the \vec{E} and \vec{H} vector

amplitudes is independent of the space variable z ; this is the quantity Z_w , called the plane wave impedance, whose value is equivalent to the square root of the ratio of the constants μ_0 and ε_0 . Z_w takes the numerical value of 377Ω or $120\pi \Omega$, if we insert into [1.11], the numerical values [1.4] allocated to μ_0 and ε_0 :

$$H_y = H_{y0} e^{-jkz} = \frac{E_{x0}}{Z_w} e^{-jkz} \quad \text{where} \quad Z_w = \frac{E_{x0}}{H_{y0}} = \frac{E_x}{H_y} = \sqrt{\frac{\mu_0}{\varepsilon_0}} \quad [1.11]$$

1.2.2. General plane wave representation

The previously established solutions aim at producing a plane wave, whose propagation direction merged with the oz axis of the Cartesian graph in Figure 1.1. This choice, which was adopted to simplify the calculations, can be extended to any propagation direction. The developments produced in section 3.3.1 of Chapter 3 show that the electric field vector \vec{E} can be linked to the position r of an observer at the origin of the graph by the following expression:

$$\vec{E} = \vec{E}_0 e^{-j\vec{k} \cdot \vec{r}} \quad [1.12]$$

In this formula, \vec{r} represents the position vector and \vec{k} represents the wave number vector, whose direction in the space specifies the propagation direction of the wave, i.e.:

$$\vec{r} = x\vec{u}_x + y\vec{u}_y + z\vec{u}_z \quad \vec{k} = k_x\vec{u}_x + k_y\vec{u}_y + k_z\vec{u}_z \quad [1.13]$$

The absolute amplitude of vector k is the scalar value defined in waves equation [1.7], i.e.:

$$|\vec{k}| = \sqrt{k_x^2 + k_y^2 + k_z^2} = \frac{\omega}{v_0} \quad [1.14]$$

In the general case, the electric and magnetic field vectors will thus have three components. Knowing that the polarization plane of the wave is normal in the propagation direction, it is easy to establish the following equations:

$$\vec{E} \cdot \vec{H} = 0 \quad \vec{E} \cdot \vec{k} = 0 \quad \vec{H} \cdot \vec{k} = 0 \quad [1.15]$$

In this general presentation, the ratio of the absolute amplitudes of \vec{E} and \vec{H} is, as previously, the impedance of the plane wave Z_w :

$$\frac{|\vec{E}|}{|\vec{H}|} = \sqrt{\frac{\mu_0}{\epsilon_0}} = Z_w \quad [1.16]$$

1.2.3. Assimilation of the far-field to a local plane wave

Let us associate a source of the electromagnetic field with the spherical coordinates in Figure 1.2. The origin o of the graph is contained in the source; we can define the unit vector \vec{u}_r , \vec{u}_θ and \vec{u}_ϕ associated with the variables r , θ and ϕ , absent from the figure; the polar axis is fixed by XX' .

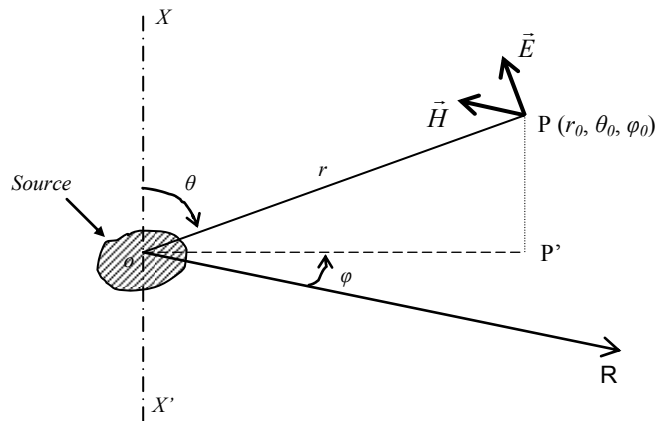


Figure 1.2. Emission source attached to spherical coordinates

The near-field zone, also called Rayleigh zone is located as a function of the distance of the observer. The zone is defined for a distance r much lower than the wavelength, but comparable to the dimensions of the source. Then, there is the Fresnel zone for distances r still lower than λ , but quite long compared to the source dimensions. And finally there is the far-field space or Fraunhofer zone for radial directions r much higher than λ .

As specified in section 6.2.1 of Chapter 6, the electric field vector \vec{E} and the magnetic field vector \vec{H} observed in the far-field remain orthogonal and their

evolution as a function of the r , θ and ϕ variables appropriates the general forms below:

$$\vec{E} = \vec{V}(\theta, \phi) \frac{e^{-jkr}}{r} \quad \vec{H} = \vec{I}(\theta, \phi) \frac{e^{-jkr}}{r} \quad \text{where} \quad \vec{E} \cdot \vec{H} = 0 \quad [1.17]$$

The functions $\vec{V}(\theta, \phi)$ and $\vec{I}(\theta, \phi)$ of the variables θ and ϕ characterize the directivity of the radiation so called the radiation pattern. These are orthogonal vectors taking respective homogeneous physical units from a voltage and a current.

We obtain a spherical wave, whose propagation direction is carried by the radial unit vector \vec{u}_r , which is normal at the polarization plane of the fields \vec{E} and \vec{H} . The amplitude ratios are only governed by the impedance of the plane wave, as shown in equation [1.18]:

$$\vec{E} \cdot \vec{u}_r = 0 \quad \vec{H} \cdot \vec{u}_r = 0 \quad \frac{|\vec{E}|}{|\vec{H}|} = \sqrt{\frac{\mu_0}{\epsilon_0}} = Z_w \quad [1.18]$$

Let us consider an observer located at point P with coordinates r_0 , θ_0 and ϕ_0 , but making a position excursion Δr , $\Delta\theta$ and $\Delta\phi$ of relatively short path. By only keeping the first terms of the series expansion of the functions $\vec{V}(\theta, \phi)$ and $\vec{I}(\theta, \phi)$, we search for \vec{E} and \vec{H} in the approximate expression [1.19]:

$$\vec{E} \cong \vec{E}_0 e^{-jk\Delta r} \quad \text{where} \quad \vec{E}_0 = \vec{V}(\theta_0, \phi_0) \frac{e^{-jkr_0}}{r_0} \quad [1.19]$$

Knowing that we find a similar form for the magnetic field vector, we can conclude that the far-field propagated on the path Δr locally obeys the physical behavior of a plane wave. This property will be used during immunity and susceptibility tests.

1.2.4. Induction phenomena produced by plane waves

We will see in the rest of the book that most of the measurements carried out in the instruments generating electromagnetic fields can be reduced to the induction mechanisms of plane waves on circuits. To simplify, we reduce the circuit to a rectangular shaped loop, L_0 in length and h in height, arranged in accordance with the diagram in Figure 1.3. A gap made between the AB points receives the load impedance R_L .

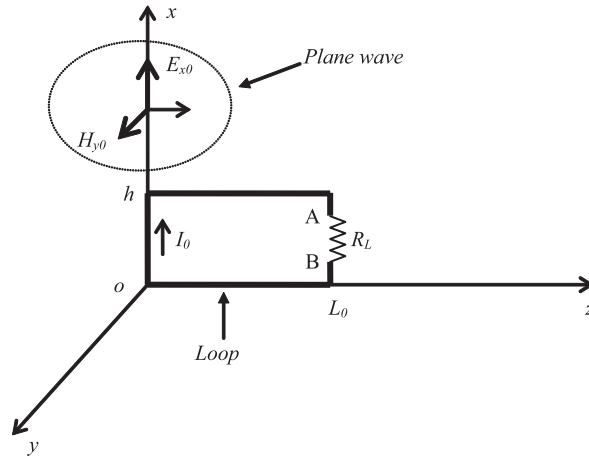


Figure 1.3. Geometrical configurations of the loop induced by the plane wave

The incoming plane wave is polarized in the oxy plane and the propagation direction is supported by the oz axis presently merged with the L_0 dimension of the loop. The electric field vector \vec{E}_0 carried by the wave at the origin of the graph, is reduced to the only component directed on the ox axis merged with the dimension h of the loop. The magnetic field vector \vec{H}_0 of the wave at the origin of the graph is thus normal to the surface S of this loop and directed according to oy .

The wave is animated by continuous sinusoidal shape under the angular frequency ω . We admit that the wavelength λ remains much higher than the largest dimension of the loop. The wave thus polarized will induce on the load impedance, a voltage V_{AB} whose amplitude will be determined with the help of an equivalent circuit shown in Figure 1.4.

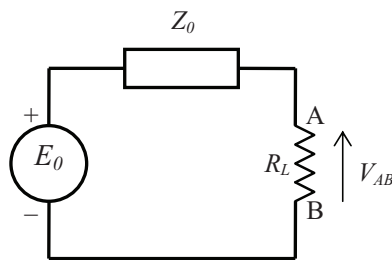


Figure 1.4. Circuit equivalent to the induction of the plane wave on the loop

In this diagram, E_0 represents the induced electromotive force (emf) and Z_0 is the internal impedance of the loop, presently reduced to a reactance.

The determination of the induced emf can be carried out in two different ways: adopting the well-known law of induction by the magnetic field vector \vec{H} ; or involving the interaction of the electric field component vector \vec{E} , projected on the conductors constituting the loop. The second calculation incorrectly called the *theory of the receiving antennas* concerns the diffraction of the fields on the wires. With the assumption of the electrical small loop, the calculations carried out in section 1.2.4.1 by the magnetic field and in section 1.2.4.2 by the electric field, lead to identical results.

1.2.4.1. Calculation by induction of the magnetic field vector \vec{H}

Before doing this elementary calculation, we must justify how the magnetic field remains invariant on the loop. For this, let us take a look at the expressions of H_y at the positions $z = 0$ and $z = L_0$, i.e.:

$$\vec{H} = H_y(z)\vec{u}_y \rightarrow H_y(0) = H_{y0} \quad H_y(L_0) = H_{y0} e^{-jkL_0} \quad [1.20]$$

By adopting the expression of the wave number containing the wavelength λ , the assumption of the electrical small loop allows use of first and second terms of the series expansion in equation [1.20] leading to the simplified form of [1.21]:

$$\lambda \gg L_0 \quad \text{and} \quad kL_0 = 2\pi \frac{L_0}{\lambda} \rightarrow H_y(L_0) \cong H_{y0} \left(1 - j2\pi \frac{L_0}{\lambda} \right) \cong H_{y0} \quad [1.21]$$

If the second term of this equation becomes negligible compared to the unit, we deduce that the magnetic field is almost invariant on the surface of the loop. After insertion of the complex notations, we draw from the Lenz law, the expression of the induced emf E_0 , i.e.:

$$h_y(t) = H_{y0} e^{j\omega t} \rightarrow e_0(t) = -\frac{d\phi}{dt} = E_0 e^{j\omega t} \rightarrow E_0 = j\omega \mu_0 H_{y0} hL_0 \quad [1.22]$$

Let us specify that approximation [1.21] brings back the calculation of the magnetic flux to the scalar product of the induction vector $\mu_0 \vec{h}(t)$ and of the surface vector \vec{S} :

$$\phi = \mu_0 \vec{h}(t) \cdot \vec{S} \quad \text{where} \quad \vec{S} = hL_0 \vec{u}_y \quad [1.23]$$

From the circuit of Figure 1.4, we easily deduce the expression of V_{AB} :

$$V_{AB} = \frac{R_L}{Z_0 + R_L} E_0 \quad [1.24]$$

1.2.4.2. Calculation by interaction of the electric field vector \vec{E}

The conditions of electrical small loop are such that the current I_0 induced on the entire loop perimeter must have a uniform amplitude. These conditions lend themselves very well to the analytical calculation of V_{AB} by the integral of the electric field vector. The vector \vec{E} has only one single projection in the direction of the ox axis and thus the conductors perpendicular to this direction will not be concerned by the calculation, since the electric field will not have an effect on these parts. We can thus summarize this simply by saying that the interaction of \vec{E} with the edges of the loop collinear to the ox axis induces the emfs designated by the $E_0(0)$ and $E_0(L_0)$. Taking into account the current uniformity, the previous emfs are reduced to the product of E_x and the dimension h , i.e.:

$$E_0(0) = E_{x0} h \quad E_0(L_0) = E_{x0} h e^{-jkL_0} \quad [1.25]$$

The diagram in Figure 1.5a shows the installation of the computed voltage sources, whose polarity is imposed by the direction of the vector \vec{E} .

The interaction shown by Figure 1.5a is reduced to the equivalent circuit of Figure 1.5b, where the source ΔE_0 must play a part similar to the E_0 emf, induced by the magnetic field vector \vec{H} .

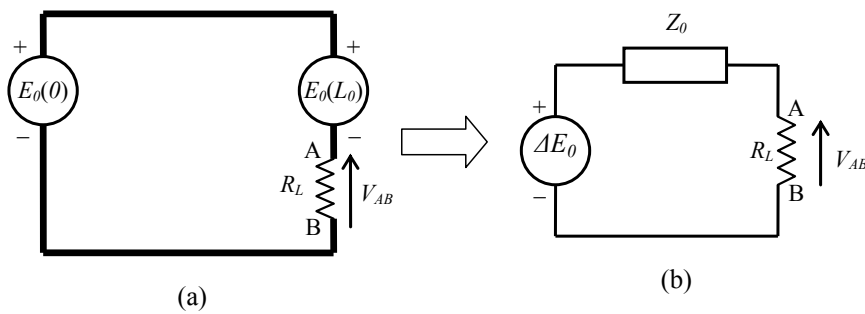


Figure 1.5. Illustration of the interaction of the loop with the electric field

Indeed, the use of relation [1.25] allows us to write ΔE_0 in the following form:

$$\Delta E_0 = E_0(0) - E_0(L_0) = -E_{x0}h \left(1 - e^{-jkL_0}\right) \quad [1.26]$$

By taking into account the electrical small loop condition, the expression in brackets can be developed in the first order to reach the approximate value of ΔE_0 :

$$\lambda \gg L_0 \rightarrow \Delta E_0 \cong j E_{x0} h k L_0 \quad [1.27]$$

After a few trivial transformations involving expression [1.7] of the wave number and the impedance of the plane wave [1.11], we search for ΔE_0 a formula strictly identical to E_0 , i.e.:

$$\Delta E_0 \cong -j\omega\mu_0 H_{y0} h L_0 \quad [1.28]$$

E_0 and ΔE_0 consequently gather only one physical phenomenon of induction, and we can thus conclude that just the knowledge of the electric field vector is large enough to evaluate the electromagnetic constraint undergone by any electronic equipment illuminated by a plane wave.

1.3. Electromagnetic tests in confined areas

The exposure of electronic equipment to the far-field emitted by an antenna certainly represents the simplest configuration in order to produce immunity or susceptibility tests. According to the developments of the previous section, we find that the far-field of an antenna amounts to a local plane wave and consecutively to the presence of an electric field, whose amplitude characterizes the level of the electromagnetic constraint. Carrying out such an experiment, however, assumes the combination of two conditions: the antenna and the object under test must be far away from any obstacle absorbing or diffracting the waves.

In other words, we seek to get close to the propagation properties encountered in the free space. This theoretical ideal cannot be carried out and thus we must come to a compromise with the contribution of elements imposed by the environment of the measurements' site. The ground is one of the first elements involved; its electric conductivity reflects the waves, and consequently produces interference generating uncertainties in the estimate of the constraint supported by the object under test. International regulations are added to this physical effect, requiring minimum emission thresholds and frequency bands imposed by the legal use of the radio space. The strict restrictions expressed on the amplitude of the electromagnetic

fields force us to confine the immunity or susceptibility tests in areas with high performance electromagnetic shields.

A similar provision is necessary during the measurement of the wide spectrum emission, observed during the usual operation of electronic equipment. Indeed, the objective of the emission tests is to detect electric fields whose amplitudes are close to the sensitivity threshold of the broadcasting receivers, which is often close to $100 \mu\text{V/m}$. Low amplitude levels are constantly jammed by emissions produced by the increasingly numerous users of the radio space. As for the practice of the immunity tests previously mentioned, reliable measurements of stray emissions can only be done in an enclosure protected by a good shielding material.

In these circumstances, the confinement of the waves inevitably has an impact on the objectivity of an electromagnetic test and on the precision of the results coming from the measurements.

Before paying attention to the uncertainties involved in reverberation chambers, including their originality with regard to this crucial question, we will examine some weaknesses encountered in other electromagnetic test devices. This will be the generation of waves carried out in TEM cells, and then in the anechoic chambers. To simplify the physical analysis of the phenomena, the object under test will be reduced to the rectangular loop described previously. We will first analyze the radiation produced by this loop.

1.3.1. *Emission of a small rectangular loop*

Let us consider the rectangular loop of dimensions $L_0 \times h$ presented this time in the context of the spherical graph in Figure 1.6. The polar axis XX' normal at the plane of the loop goes through its geometrical center.

The radiation theory of the antennas, exposed in Chapter 6, gives access to three formulas expressing the electric field vector \vec{E} and the magnetic field vector \vec{H} as a function of the variables r , θ and φ . The formulas, whose complete expressions are not detailed, assume that two simultaneous conditions will be taken into account: the P observer must be located at a much higher distance r from the loop than the dimensions L_0 and h ; the current I_0 must be uniformly distributed on the perimeter of the loop. The second condition thus means that the wavelength must be much longer than the dimensions L_0 and h :

$$r \gg L_0, h \quad \text{and} \quad \lambda \gg L_0, h \quad [1.29]$$

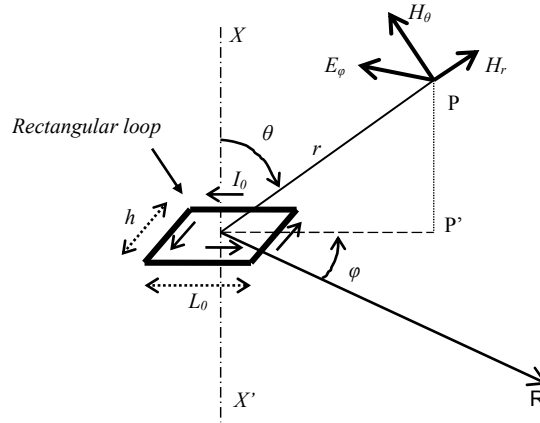


Figure 1.6. Spherical coordinates attached to the emission of a small loop

The calculation gives two components of the magnetic field vector, respectively directed according to the radial and polar directions. Only one component of the electric field vector is directed according to the angular coordinate ϕ , i.e.:

$$\vec{H} = H_r \vec{u}_r + H_\theta \vec{u}_\theta \quad \vec{E} = E_\phi \vec{u}_\phi \quad [1.30]$$

We will examine the approximate formulas established for the near-field (Fresnel zone) and for the far-field (Fraunhofer zone).

1.3.1.1. Near-field Formulas

With the hypothesis that the position r of the observer is much lower than the wavelength, the approximate formulas of the components of vectors \vec{E} and \vec{H} are expressed with the following relations:

$$r \ll \lambda \rightarrow H_r \cong \frac{m}{4\pi} \frac{2 \cos \theta}{r^3} \quad H_\theta \cong \frac{m}{4\pi} \frac{\sin \theta}{r^3} \quad [1.31]$$

$$r \ll \lambda \rightarrow E_\phi \cong -j\omega \frac{m \mu_0}{4\pi} \frac{\sin \theta}{r^2} \quad [1.32]$$

The coefficient m in these relations is called the magnetic moment. This is the product of the current I_0 and the surface S of the loop:

$$m = I_0 S \quad \text{with} \quad S = hL_0 \quad [1.33]$$

As shown by the expression below, the wave impedance attached to the near-field is purely reactive. Moreover, we find in this formula the impedance of the plane wave Z_w :

$$\frac{E_\phi}{\sqrt{H_r^2 + H_\theta^2}} = -j\omega \frac{r}{c} \frac{\sin \theta}{\sqrt{1 + 3 \cos^2 \theta}} Z_w \quad [1.34]$$

In this relation, there is also the celerity c , meaning the loop is installed in the free space.

Expression [1.34] shows that the wave impedance is almost zero when the angular frequency ω of excitation gets close to zero. This remarkable property means that, close to the loop, the emission is due to the magnetic field. We have here a heterogeneous wave, whose amplitude ratio of the vectors \vec{E} and \vec{H} depends on the angular frequency and on the geometrical variables r and θ .

1.3.1.2. Far-field formulas

For an observer located at a distance r from the loop much higher than the wavelength, we can show that the radial component of the magnetic field gives way to the polar component:

$$r \gg \lambda \rightarrow H_r \ll H_\theta \quad [1.35]$$

Consequently, for the far-field, the components H_θ and E_ϕ are the only ones remaining whose approximate expressions appropriate the following analytical formulas:

$$r \gg \lambda \rightarrow H_\theta \cong \omega^2 \frac{m}{4\pi c^2} \frac{e^{-jkr}}{r} \sin \theta \quad E_\phi = Z_w H_\theta \quad [1.36]$$

We find the properties of the local plane wave stated in section 1.2.3.

1.3.2. Tests carried out in a TEM cell

The TEM cell forms a confined enclosure in which we manage to produce electromagnetic constraints close to the properties of the plane wave. The TEM cell can also measure the emission of objects. The only restrictions of use are related to taking into account the approximation of the TEM (transverse electromagnetic)

propagation, as well as the volume of the test objects with respect to the volume of the cell.

Figure 1.7 reproduces the diagram of the longitudinal and transversal sections of a typical TEM cell [DEM 04].

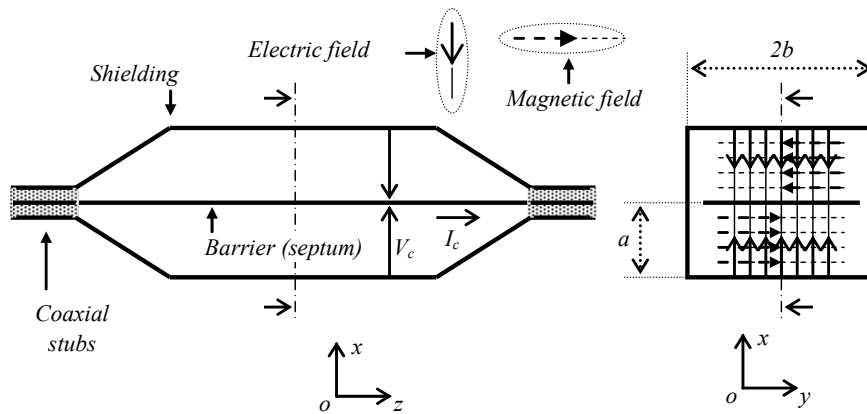


Figure 1.7. Brief description of a TEM cell

The device is a coaxial structure of rectangular section; the outer metal envelope plays a shielding role, whereas the inner metal plane is the active element of the cell, often designated by the term septum. Coaxial transitions located at both ends help to connect several instruments. We propose briefly analyzing the functioning of this device during an immunity or emission test.

1.3.2.1. Carrying out an immunity test

The emission source can be connected to the left termination of the cell, while a matched load is connected to the other termination, in order to generate a forward wave. With the condition that the wavelength remains much longer than the transversal dimensions $2a \times 2b$, we can show that a transverse electromagnetic wave propagates in the longitudinal direction oz . For an observer located in the zone mentioned on the right side of Figure 1.7, the TEM wave will be characterized with a predominant component E_x of electric field vector directed (or falling) towards the cell plane. With these conditions, the amplitude of E_x is almost invariant with the transversal coordinates x and y . The TEM wave also carries a magnetic field vector, whose main component H_y , which is parallel to the ground plane, also remains only mildly dependent on the x and y variables. Because of these properties, the TEM wave can be locally assimilated to the propagation of a plane wave. To carry on with

the analysis will however show that in the presence of an object, the assimilation to the plane wave concept leads to uncertainties generated by the energy confinement.

Taking into account the hypotheses stated previously, the electric field vectors \vec{E} and the magnetic field vectors \vec{H} are expressed with the following notations:

$$\vec{E} = E_x \vec{u}_x \quad \vec{H} = H_y \vec{u}_y \quad [1.37]$$

Knowing that the high frequencies source applies the voltage V_c between the septum and the shielding, a satisfying approximation of the amplitude of the electric field E_x can be taken from the formula recalled below for the plane capacitor:

$$E_x \cong \frac{V_c}{a} \quad [1.38]$$

The geometrical parameter a represents the distance between the septum and the ground plane of the cell.

The cell is matched at the right termination, i.e. connected to its own characteristic impedance Z_c , and thus the current I_c attached to the TEM wave produces a magnetic field vector, whose main component H_y is linked to the current by the proportionality coefficient K_H , i.e.:

$$I_c = \frac{V_c}{Z_c} \quad \text{with} \quad H_y = K_H I_c \quad [1.39]$$

With the assumption of the TEM propagation, the \vec{E} and \vec{H} vectors are orthogonal and the amplitude ratio is none other than the impedance of the plane wave, hence:

$$\frac{|\vec{E}|}{|\vec{H}|} = Z_w = \sqrt{\frac{\mu_0}{\epsilon_0}} \cong \frac{E_x}{H_y} \quad [1.40]$$

The K_H coefficient can thus be found after combining the previously established relations.

Let us now consider the rectangular loop immersed in the cell with the direction previously defined in Figure 1.3. The loop will be the place of an induced emf E_0 , determined by expression [1.41], taken from the induction law:

$$E_0 = j\omega\mu_0 H_y S \quad [1.41]$$

In this context, the induced emf can be calculated differently, by saying it results from the mutual inductance L_m exerted between the TEM cell and the loop, i.e.:

$$E_0 = j L_m \omega I_c \quad [1.42]$$

The absence of the negative sign in expressions [1.41] and [1.42] is justified, in order to have these relations comply with the directions used in Figure 1.9. The I_c current injected in the TEM cell is in expression [1.42]. With the use of relations [1.39] and [1.41], we find that L_m is connected to the K_H coefficient by the following expression:

$$L_m = \mu_0 K_H S \quad [1.43]$$

In reality, an electric coupling generated by the component E_x is added to the coupling exerted by the magnetic field. This phenomenon comes from closing the lines in the electric fields via the horizontal conductor of the loop the furthest possible from the ground plane. To illustrate this additional coupling, Figure 1.8 describes the loop connected to the load resistor R_L by a coaxial cable, whose shielding is connected to the ground plane of the cell.

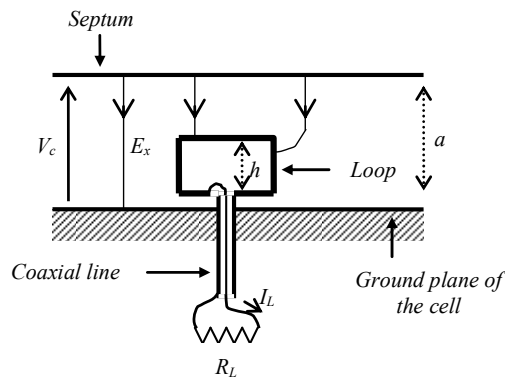


Figure 1.8. Illustration of the electric cross-coupling generated by V_c

The presence of the object thus connected to the metal ground plane locally distorts the lines of the electric field. We witness the induction of charges by electric coupling, whose flow is mainly carried out via direct contact with the ground shielded plane. However, a small part of the coupled electric charges flows through

the inner wire of the coaxial cable and consecutively through the resistor R_L . These charges generate the current I_L that we may link to the voltage V_c applied to the cell through a mutual capacitance C_m :

$$I_L = j C_m \omega V_c \quad [1.44]$$

When the dimension h of the object remains much lower than the distance a , the capacitance C_m is negligible and the coupling exerted by the TEM wave is thus very close to the induction carried out by a plane wave. This coupling is calculated in a rigorous way as depicted in section 1.2.4. Let us specify that the calculation of the interaction of the electric field component, done in section 1.2.4.2, is really unfamiliar to the coupling related by formula [1.44].

The electric coupling produced by C_m finally introduces a systematic error during the capture of the voltage induced on the resistance R_L . We immediately realize that this factor risks altering the reproducibility of the immunity tests carried out in the TEM cells of different dimensions. We also perceive through this simple example that the wiring topology of the object can influence the reproducibility of the tests. We will see in the following sections that other devices, generating electromagnetic waves in a confined area generate systematic errors of their own.

1.3.2.2. Measurement of the emission in a TEM cell

The emission measurement consists of capturing the power collected at both ends of the TEM cell during the inner coupling given by a radiating object. The use of the loop illustrated in Figure 1.6 will again facilitate the physical interpretation.

Indeed, let us consider, as previously, the loop arranged perpendicularly to the ground plane as well as to the transversal section of the TEM cell. The injection of the current I_0 will locally produce a magnetic field that induces an emf E_c . By assuming the cell is matched at both ends, this emf E_c takes place in the equivalent circuit of Figure 1.9.

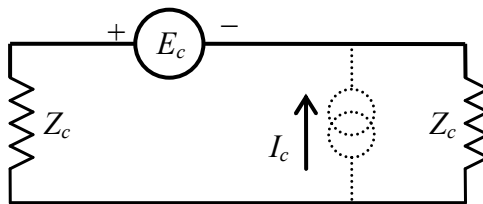


Figure 1.9. Equivalent circuit of an emission measurement carried out in a TEM cell

By applying the reciprocity theorems, E_c is easily deduced from equation [1.45] which includes the injected current I_0 , as well as the mutual inductance L_m defined in [1.43]:

$$E_c = j L_m \omega I_0 \quad [1.45]$$

Knowing that the loads Z_c connected on the cell are purely real, the P_c power collected during the loop emission is thus determined by the sum of the powers dissipated in these two resistors, i.e.:

$$P_c = \frac{|E_c|^2}{2Z_c} \quad [1.46]$$

To be rigorous, we must add the dissipated power in the septum and the TEM cell shield. The latter is generally much lower than P_c .

A more detailed reasoning proves that the power P_c has no link with the radiated power by the loop in free space. Indeed, the radiated power comes from the flux of the Poynting vector, calculated on a spherical surface centered on the loop. This is the active power carried by the far-field, whereas P_c results from the conversion of the near magnetic field in induced power.

In keeping with the discussion started about the error generated during the immunity test, the P_c measurement is also concerned by a systematic error, due to the electric coupling occurring between the loop and the septum. This phenomenon is transposed in the diagram in Figure 1.9 by the current source I_c (dotted line). By reciprocity, we can calculate the current I_c thanks to equation [1.47] in which we find the coupling capacitance C_m and the voltage V_B applied to the loop by the source generating the I_0 current, hence:

$$I_c = j C_m \omega V_B \quad [1.47]$$

The positive sign adopted in this expression is justified by the choice of the direction of the current source in Figure 1.9. If the loop has sufficiently low impedance, the voltage V_B will be of very low amplitude. This factor will thus reduce the current contribution I_c , without however completely eliminating it. From this electric coupling a systematic error will result in the measurement of the loop emission.

1.3.3. Measurements carried out in an anechoic shielded chamber

As mentioned above, the production of local plane waves is possible by immersion of the object in the far-field coming from a wide frequency range antenna. The field must be confined in a shielded enclosure whose dimensions are necessarily dependent on the radius of the Fraunhofer zone of the emitting antenna. If we wish to do an immunity test using this process at the frequency of 100 MHz, the distance separating the antenna from the object under test must thus be much longer than the wavelength, presently equal to 3 m. In general and for this frequency, we set the minimal distance at 10 m. This criterion will thus impose the volume of the shielded chamber and consequently its cost!

The distance is initially set at 10 m requiring chambers of prohibitive volume. The antenna-object distance suggested in the normative protocols has been reduced to 3 meters. This dimensional constraint has an immediate impact on the appearance of the far-field condition between 200 MHz and 300 MHz. In order to find the propagation of waves getting close to the free space, the waves impacting on the high conductive walls of the chamber will be absorbed by the installation of suitable materials. These latter generally form a mosaic constituted of polyurethane pyramids loaded with carbon powder and stuck to the inner walls of the chamber. The thickness of the coating determines the minimal absorption frequency. For convenience reasons, the metal ground plane of the chamber does not have any absorbent, which leads us to think that we have here semi-anechoic chambers and not completely anechoic chambers, as the title of this section would lead us to think.

In the nominal conditions of an immunity test, the object under test is installed on a revolving plate, in order to seek the maximum sensitivity facing the local plane wave emerging from the emitting antenna. The position of the antenna can also be modified during a test, so that the wave polarization has an electric field vector normal or parallel to the ground plane. We then speak about vertical or horizontal polarization. Indeed, a line of reasoning based on an object made up of the small magnetic loop indicates that as a function of the wave polarization coming from the antenna, the electric field vector can be, in extreme cases, parallel to the conductors constituting the loop or on the contrary, perpendicular to the rectangular surface of this loop.

The test in an anechoic chamber requires a preliminary calibration process. This is generally the substitution method. An electric field sensor is installed in the place that the object will occupy during the immunity test. The power applied on the emitting antenna is adjusted so that the electric field amplitude fits with the required level for the immunity test. Depending on the strictness of the test, the electric field amplitude can be between 1 V/m and 30 V/m or even more. By moving the sensor in the volume that will be occupied by the object, we verify that the amplitude

variations of the field remain contained in a tolerance interval set by an international standard. Taking this criterion into account guarantees the reproducibility condition of an immunity test carried out in an anechoic chamber.

Indeed, many physical factors dependent on the arrangement of the object under test can influence the reproducibility of the measurements. We just mentioned the tolerance of uncertainty during the emission of the field set by the calibration procedure. This error originates from the behavior of the wave coming from the emission antenna, whose spatial dispersion does not respect the rigorous properties of a plane wave. To this first defect, we can add the influence of the metal ground plane of the chamber. Indeed, the object will see the field resulting from the interference of the direct wave, coming from the emission antenna and from the wave reflected off the ground. This phenomenon creates a standing residual wave carrier of amplitude variations. To these field amplitude irregularities, we can add the residual waves reflected off the absorbing materials, whose superposition to the direct wave of the antenna will produce secondary standing waves, also generating amplitude fluctuations.

Other factors are mixed with the uncertainties of the calibration. We mentioned in the previous section the electric coupling exerted on the rectangular loop tested in the TEM cell. We witness a similar behavior under the field coming from the antenna installed in an anechoic chamber. Let us imagine the ideally floating loop, i.e. connected to the load resistor R_L without any physical link to the outside environment. Under these ideal conditions, the object will be impervious to the electric field normally polarized on the loop plane. Conversely, as soon as the resistor is connected to the loop via a coaxial cable or any other wiring link, the presence of this conductor leads to an electric coupling, whose evaluation is hardly predictable. This phenomenon leads to another uncertainty source, characterized by the shift of the sensitivity threshold of the object. Knowing that the installation topology is often dependent on the inner arrangement of the chamber, the uncertainty will impact on the reproducibility of a test. By application of the electromagnetic reciprocity principle, what was just said about the immunity test can be extended to the measurement of the radio emission, coming from a electronic equipment.

1.3.4. Position of the reverberation chambers in tests carried out in a confined space

Examining the processes of tests carried out in a TEM cell and in an anechoic chamber, has shown that the confinement of the electromagnetic waves was the cause of systematic measurement errors. These relative errors, generally lower than 30%, but hardly predictable, form the uncertainty margins specific to each

instrument. In contrast with the previous methods, the mode-stirred reverberation chambers maintain waves whose amplitude will be naturally basking in the glow of an uncertainty. This natural error margin due to the feature of the field found in reverberation room will be compared with a value which corresponds to a tolerance fixed by a standard. Consequently, the calibration of the reverberation room consists of measuring the uncertainty of the electromagnetic field's amplitude according to a standardized procedure.

1.3.4.1. Immunity test confined in a reverberation chamber

Let us consider a rectangular cavity, made up of high conductive walls reflecting the electromagnetic waves. A radio frequency source connected to a very directive antenna produces a beam similar to a local plane wave. Figure 1.10 gives a brief description of this device, where S represents the surface of the beam containing the electromagnetic field related to a plane wave.

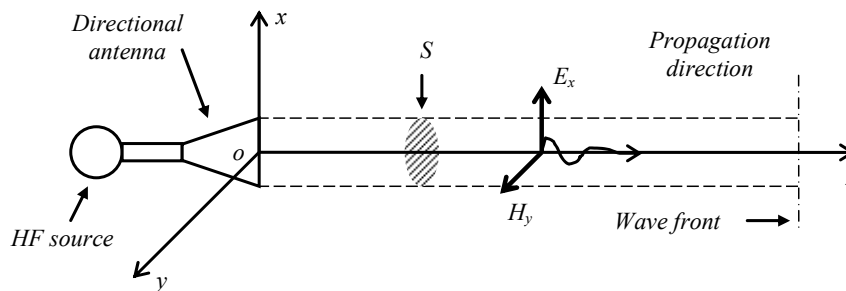


Figure 1.10. Illustration of a wave beam

With the prior hypothesis that the wavelength of the radio emission is much lower than the chamber dimensions, the confinement of the radiation will be accompanied by countless beams reflected on the walls. If we assume the walls as perfect conductive material, an observer located at any point of the chamber will have a certain probability of being intercepted by the wave front. If we modify the direction of the beam, this probability can be increased so that the interception is carried out with certainty. Intuitively, we realize that this condition can also be found for other directions scanning the solid angle of 4π and that these instances will be all the more likely as the wavelength is reduced compared to the dimensions of the chamber.

If we take into account that the walls are made of non-perfect conductive material like copper or steel, the electromagnetic field propagated in the chamber will appear in the form of standing waves. We will then witness periodic variations in the amplitude of the field which increase as the wavelength is reduced. We then

observe that the average amplitude of the field collected in the chamber becomes independent of the direction of the beam; the radiation pattern of the antenna seems to be isotropic. Thanks to the reciprocity principle, this property can be extended to the receiving antenna and *a fortiori* to any other object installed in the chamber. Consequently, the field generation process is truly different from what was done in a TEM cell and in an anechoic chamber.

If we take a more careful look at the field distribution in the reverberation chamber, we observe that the condition of oversizing compared to the wavelength has a resounding impact on the presence of objects diffracting the waves. The conditions imposed by metal objects are such that the distribution in amplitude of the standing waves is deeply modified and it thus becomes practically unpredictable. An uncertainty remaining independent from the geometry of this cavity is superimposed on the average field amplitude installed in the chamber – the only condition required to satisfy this property is oversizing compared to the wavelength. Contrary to the tests carried out in a TEM cell or in an anechoic chamber, the calibration processes of the field done in a reverberation chamber will thus naturally integrate the uncertainty generated by the objects.

In practice, this is not that simple, insofar as there are no ideally directional antennas and as it is necessary to produce waves with a stochastic behavior; the modes stirrer will carry out these conditions. As we will see in Chapter 2, the reverberation chamber is an electromagnetic cavity generating many resonances so called modes, whose properties stimulate the standing wave amplitude. The mode stirrer, made up of metal blades moving in rotation, thus aims to agitate the resonance frequency of the modes. A random distribution of the electromagnetic field results from this phenomenon. Understanding the functioning of the reverberation chamber thus cannot be accomplished after an in-depth analysis of the properties of the stochastic distribution of the field. These properties require the knowledge of some elements of the probabilities theory, recalled in Appendix 1.

1.3.4.2. *Brief description of a mode stirred reverberation chamber*

Figure 1.11 shows the main technological components of a reverberation chamber, for which we will specify the respective functions.

The chamber, made up of an assembly of metal panels in steel or copper, must have a very good shield against the electromagnetic waves. As we will see throughout the book, the power losses in the metal walls reduce the quality factor of this cavity and consecutively, the performances of the mode stirring. The aptitude for producing high fields with a low contribution of transmitting power is also influenced by the quality factor. In order to reduce the losses, the internal power supply network will be protected by an appropriate shielding. A low-pass filter will complete this network, in order to reduce the conducted disturbances. The object

under test will be moved away from the metal ground plane by an insulation support. We will keep watch, so that the material constituting this support will not locally absorb the waves, in order to preserve the quality factor of the enclosure. The output data of the operating state of the electronic equipment under test will be captured by an optical fiber, designed to reduce the risks of electromagnetic contamination. The mode stirrer will be driven by a motor, usually positioned outside the chamber. The high frequency emission source will be installed outside the chamber and the emission antenna will preferably be directional and as compact as possible, in order to reduce the direct electromagnetic couplings with the object under test and the mode stirrer.

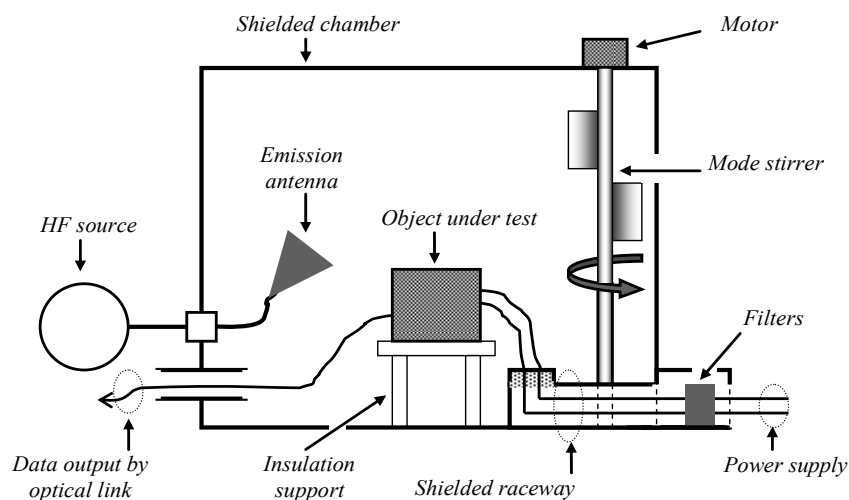


Figure 1.11. Brief description of the main components of a reverberation chamber

1.4. Discussion

1.4.1. On the use of the plane wave concepts

As explained in this chapter, the plane wave concepts can reveal some defects of the test methods based on the confinement of the electromagnetic waves. In addition to this advantage, we will show in the next chapter that any field distribution contained in a shielded room can be represented by a plane wave spectrum. Compared to the modal representation, the plane wave spectrum is better adapted to the oversized cavities, compared to the wavelength. This is notably the case when we seek to simulate the behavior of an ideal reverberation chamber with a disordered field distribution.

Evidently, other situations are less adapted than those previously described to the use of this concept, such as the description of the waves coming from more or less isotropic radiation sources. Except for the emission of the far-field within a small solid angle, where the comparison to the plane waves is still available, the extension of this concept to the description of the spherical waves or of the near-field is not at all appropriate. We will see in Chapter 6, exclusively devoted to the measurement of objects' emission that the use of series expansion made up of spherical harmonic functions will be more convenient for characterizing the radiation sources, sometimes reduced to arrangements of multipoles.

1.4.2. On the uncertainty margin of the measurements carried out in a reverberation chamber

In section 1.3.4, we showed that the knowledge and the respect of the uncertainty margin of the amplitude of the electromagnetic fields generated in a reverberation chamber justify the criteria of experiment reproducibility. Indeed, it will be shown in the following chapters, especially in Chapter 3, that the production of a random distribution of the field, with in addition the standard deviation of its average amplitude, enables us to set an uncertainty margin. The calibration of a chamber will thus require first the evaluation of the standard deviation of an average amplitude, in order to relate (or compare) it to a reference value, found in the standardized measurement procedures.

The determination of the uncertainty margin thus defined will be the result of average computation, established on the assumption of the large numbers law. Performing measurements will thus require the collection of a sufficient sample of statistically substantial data. Depending on the circumstances, it can be the amplitude of the voltages collected on a field sensor or amplitudes of power induced on a receiving antenna. In the context of the large numbers law, the data will be related to the features of *independent events* and *stationary processes*.

The term “independent events” means that a measurement must form a sample of a sufficient size N , in order to help in the construction of a histogram to compare with a known probability distribution. When we repeat the experiment in chambers of different volumes or physical constitution, the samples are assumed to fulfill the stationary condition, if the probability distribution remains unmodified. Only the gathering of these two conditions leads to the approval of the natural uncertainty margin of the chamber.

It is obvious that the insertion of objects subjected to electromagnetic tests can as a consequence have an influence on the stationary features, and in some extreme cases, the objects may produce some correlation between the collected data. In other

words, the natural uncertainty is mixed with a systematic uncertainty due to the presence of objects. The reproducibility of measurements carried out in a reverberation chamber can thus only be organized with the assistance of additional uncertainties, hidden in the official margin observed during calibration. We will see in Chapter 7 that determination of the attenuation given by the shielding of the cables or of the connectors takes this criterion into account quite well. Indeed, the topology adopted for this type of measurement assumes that the device under test is connected to the receiver outside the chamber by means of connecting cables. We can then consider the dimensions of these cables to be much more important than the device under test. Fortunately, we can show that the uncertainty generated by these long cables compared to the size of the device is located under the natural uncertainty margin of the chamber, as soon as they become oversized compared to the wavelength. Their impact should thus be without a significant influence on the reproducibility of the measurements of shielding attenuation.

1.5. Bibliography

- [DEM 04] DÉMOULIN B., *Initiation à la compatibilité électromagnétique*, vol. II, Essais et Mesures, Course notes, Second year Masters, Lille 1 University, September 2004.
- [ESU 81] *Encyclopédie Scientifique de l'Univers: La Physique*, Bureau des longitudes et Gauthier-Villars, Paris, 1981.
- [HAR 61] HARRINGTON R.F., *Time Harmonic Electromagnetic Fields*, McGraw-Hill, New York, 1961
- [UZA 05] UZAN J.-P., LEHOUCQ R., *Les Constantes Fondamentales*, Belin, Paris, 2005.